

Nonlinear photomagnetization in insulators

Bernardo S. Mendoza,^{1,2} Norberto Arzate-Plata,¹ Nicolas Tancogne-Dejean,² and Benjamin M. Fregoso³

¹*Centro de Investigaciones en Óptica, A.C., León, 37150 Guanajuato, Mexico*

²*Max Planck Institute for the Structure and Dynamics of Matter, Luruper Chaussee 149 Hamburg, Germany*

³*Department of Physics, Kent State University, Kent, Ohio 44242, USA*

Nonlinear photomagnetization is a process by which an oscillating electric field can induce a static magnetization. We show that all 32 crystallographic point groups admit spin polarization to second order using circularly polarized electric fields (as in the usual spin orientation) but only 29 points groups admit spin polarization to second order using linearly polarized electric fields. The excluded point groups are the highly symmetric $m-3m$, $-43m$ and 432 . To illustrate our results, we compute the second order electric spin susceptibility of Te, Se, SnS₂, GaAs, InSb and Si using density functional theory which corresponds to nonmagnetic materials with and without inversion symmetry. We show that our nonlinear photomagnetization can reach magnetic moments of $0.39 \mu_B$ /atom comparable to those of naturally occurring ferromagnets.

Introduction: Control over materials' magnetization finds important technological applications in data storage, memory reading/writing, and quantum information[1–8]. Materials chosen for applications usually do not have inversion or time-reversal symmetry because the ground state of such materials has spin-degenerate bands[9–11]. This limitation is partially lifted if excited states are involved. It is possible to generate a macroscopic spin polarization using electric fields[4–8] in the nonlinear regime[12–37]. In this case one is usually confined to use circularly polarized electric fields (CPE) to obtain a finite spin polarization[36]. The usual mechanism is the angular momentum transfer from photons to electron' spin[7, 8], e.g. spin inverse Faraday effect; a linearly polarized electric field (LPE) would not induce a spin polarization since it carries no angular momentum. Here we show rigorously that *all* materials can be spin-polarized by CPE (as expected) but a large class of materials also admit spin polarization by LPE.

Angular momentum is not conserved in the presence of spin-orbit coupling (SOC), yet SOC allows access to electrons' spin degrees of freedom via LPE. To balance angular momentum, other degrees of freedom pick up angular momentum because of internal torques[38]. This should be compared and contrasted with the usual spin orientation effects using CPE, which, in a sense, already breaks \mathcal{T} obviating the need for magnetic materials or SOC. In a sense, a LPE (in the nonlinear regime) breaks time-reversal symmetry (\mathcal{T}) or inversion symmetry (\mathcal{I}) *dynamically*. Here we show rigorously that all materials can be CPE spin polarized regardless of the existence of \mathcal{T} or \mathcal{I} , and for a large class of materials LPE-spin polarization is forbidden.

In addition, we provide real material examples of optical LPE spin polarization in *nonmagnetic centrosymmetric* insulators and compare with usual spin orientation effects. Our work highlights a hitherto unexplored novel control knob, the light polarization, of electron's spin.

Symmetry constrains: Consider an expansion of a

macroscopic *pseudo-vector* $\bar{\mathbf{V}}$ (e.g., spin polarization) to second order in a perturbation \mathbf{V} (e.g., electric field)

$$\bar{\mathcal{V}}^a(\omega) = \zeta^{abc} V^b(\omega) V^c(-\omega). \quad (1)$$

where $\mathbf{V}(\omega)$ is the Fourier component of the time-dependent, monochromatic perturbation at frequency ω

$$\mathbf{V} = \mathbf{V}(\omega) e^{-i\omega t} + c.c.. \quad (2)$$

$\bar{\mathbf{V}}$ is time-independent and ζ is a third-rank pseudotensor, where a, b, c are Cartesian coordinates. For conciseness we omit all frequency dependance in subsequent equations. Summation over repeated indices is implied. In metals the leading contribution to spin polarization is linear (Edelstein effect) but in insulators Eq. 1 is the leading contribution.[39]

A transformation of the coordinate frame by an element M of the crystallography point group of the crystal should leave the physical response invariant (up to some reshuffling of indices). This imposes the constrains

$$\zeta^{a'b'c'} = \det(M) M^{aa'} M^{bb'} M^{cc'} \zeta^{abc}, \quad (3)$$

where $\det(M)$ introduces a negative sign for improper transformations. In the case of the observable being a vector \mathbf{V} instead of a pseudovector, we have to second order

$$\mathcal{V}^a = \chi^{abc} V^b V^c, \quad (4)$$

where χ is a third-rank tensor with transformation law

$$\chi^{a'b'c'} = M^{aa'} M^{bb'} M^{cc'} \chi^{abc}. \quad (5)$$

If the point group does not contain improper transformations the factor $\det(M)$ is irrelevant and the tensor and pseudotensor have the same symmetry constrains. If the point group contains improper transformations the symmetry constrains can be profoundly different as shown below. In Table II, we show the nonzero components of ζ and χ after imposing the symmetry constrains of the

TABLE I. Characters table of the group. See main text for details.

Class	$\chi^{(1)}$	$\chi^{(2)}$	$\chi^{(3)}$	$\chi^{(4)}$
$C_1(I)$	1	1	1	1
$C_2(S)$	1	1	-1	-1
$C_3(A)$	1	-1	1	-1
$C_4(SA)$	1	-1	-1	1

32 crystallographic points groups. As expected, the presence of inversion symmetry force all components of the tensor to vanish[40] while the components of the pseudotensor are finite. Even if there is no \mathcal{I} , the nonzero Cartesian components are different in 8 point groups: -4 , $4mm$, $-42m$, $3m$, -6 , $6mm$, $-6m2$, $-43m$. This distinction is more evident if we separate the symmetric and antisymmetric part as (schematically)

$$\bar{\mathbf{V}} = \nu_2 |\mathbf{V}|^2 + v_2 \mathbf{V} \times \mathbf{V}^*, \quad (6)$$

$$\mathbf{V} = \sigma_2 |\mathbf{V}|^2 + \eta_2 \mathbf{V} \times \mathbf{V}^*, \quad (7)$$

where by definition $\nu_2(\sigma_2)$ is symmetric in the V -field indices and $v_2(\eta_2)$ is antisymmetric in the V -field indices. Clearly, we can always decompose a 3rd-rank tensor (pseudo-tensor) in this way, which implies that ζ is complex with $\nu_2 = \text{Re}(\zeta)$, $v_2 = i\text{Im}(\zeta)$, and $(\zeta^{abc})^* = \zeta^{acb}$. Likewise, σ_2, η_2 and χ satisfy similar constrains.

The nonzero components of ν_2, v_2 (or σ_2, η_2) can be found simply by inspection of Table II, but it is interesting to consider the problem more formally. The nonzero components of the 3rd-rank tensor (pseudo-tensor) form a representation of the group of transformations $G = \{I, S, A, AS\}$ where I is the identity, $S : (abc)^* \rightarrow acb$, A identifies components according the symmetry constrains. Because $S^2 = A^2 = (AS)^2 = I$, the group has four one-dimensional irreducible representations $D^{(1)}, \dots, D^{(4)}$ with character table shown in Table I. Any representation of G can be decomposed as

$$D = c_1 D^{(1)} \oplus c_2 D^{(2)} \oplus c_3 D^{(3)} \oplus c_4 D^{(4)} \quad (8)$$

where $c_1 + c_2$ ($c_3 + c_4$) is the number of symmetric (antisymmetric) combinations and c_1 (c_3) gives the number of distinct nonvanishing such components, i.e., the number of distinct components of ν_2 (v_2). Using Table I and II and we find the c_i for all the tensor and pseudotensor representations of G . In the Supplementary Information (SI) we explicitly show these components.

Physically, ν_2 and σ_2 determine the response to LPE whereas v_2 and η_2 determine the response to CPE. For example, it is easy to show that the former vanishes for CPE and the latter vanishes for LPE. In other words, ν_2 is independent of the ellipticity of light. This decomposition provides information about whether a material supports spin polarization via CPE, LPE, CPE or LPE, or neither. As an example consider spin polarization in response to an electric field. From Table II we see that *all*

32 points groups admit spin polarization via CPE (usual spin orientation, inverse spin Faraday effect), but only 29 admit it with LPE. The points groups $m-3m$, $-43m$, and 432 do not allow spin polarization under LPE because $\nu_2 = 0$. Also, there are 3 points groups that only admit vector symmetric response ($-43m$, $-6m2$, -6) and one point group that only admits vector antisymmetric response (432).

As another example consider the current response to an electric field to second order in perturbation theory. The above analysis shows that 3 (and only 3) point groups admit shift current[41–51] (and no injection current) whereas one (and only one) point group admits injection current (and no shift current). GaAs (point group $-43m$) would be an example of the latter which, as is well-known, admits injection current only [52] and no shift current. As a third example, consider electric polarization response to an electric field to second order in perturbation theory. Our results show that GaAs exhibits LPE second harmonic generation only.

Materials with \mathcal{I} and \mathcal{T} , e.g. materials with point groups $m-3$, $6/mmm$, which respond to LPE spin polarization, have different mechanism than conventional spin orientation effects [7, 53]. As shown in the SI, in this case the response tensor ν_2 does not vanish and depends on off-diagonal elements of the density matrix. This means it is a pure quantum effect that requires interband coherence. Intuitively, we can think of the spin-up and spin-down states at a \mathbf{k} -point precessing at slightly different directions due to the local effective magnetic field enabled by SOC. Addition of all such spins gives a net polarization if their phases are coherent. For highly symmetric crystals addition of spins cancels.

Our present results also give more insight into the materials studied recently in Ref. [54]. For example *BiH* has point point $-3m$ and hence allows LPE(CPE) spin polarization with 2 components $xxx = -xyy = -yyx, xyz = -yxz$ ($xyz = -yxz, zxy$). We now present concrete examples that prove our points above.

Materials: Te: As a first example consider Te (point group 32) which has spin-split bands and is widely used in technological applications. A decomposition of the spin pseudotensor into symmetric and antisymmetric parts gives 2 distinct symmetric components $\nu_2^{xxx} = -\nu_2^{xyy} = -\nu_2^{yyx}$, and $\nu_2^{xyz} = -\nu_2^{yzx}$ and two distinct antisymmetric components $v_2^{xyz} = -v_2^{yxz}$, and v_2^{zxy} . Therefore, Te admits both CPE and LPE spin polarization. Let us consider a LPE in the xy -plane as $\mathbf{E} = (\cos \phi, \sin \phi, 0)E_0 \cos \omega t$ where ϕ is the angle with respect to x -axis and E_0 is the electric field amplitude. In this case the spin is also on the xy -plane and given by

$$\mathbf{S}^{\leftrightarrow} = (\cos 2\phi, -\sin 2\phi, 0)S_0^{\leftrightarrow}. \quad (9)$$

where $S_0^{\leftrightarrow} = E_0^2 \nu_2^{xxx} / 2$ is the spin amplitude. A rough estimate of the magnetization is $M_0^{\leftrightarrow} = 2\mu_B S_0^{\leftrightarrow} / \hbar$ (see SI), with μ_B the Bohr magneton. The in-plane electric

TABLE II. Nonzero components of a third-rank tensor and pseudotensor for all the 32 crystallographic point groups. The external perturbation is assumed to be a vector, e.g., electric field. Also shown are the number of symmetric (σ_2/ν_2) and antisymmetric (η_2/ν_2) distinct components in each case, respectively.

Point group	tensor			pseudo-tensor	
		σ_2	η_2	ν_2	ν_2
1	all	18	9	all	18 9
-1	-	0	0	all	18 9
2	$xzx, xzy, xxz, xyz, yxz, yzy$ $yyz, yzx, zxx, zxy, zyx, zyy, zzz$	8	5	same	8 5
m	$xzx, xzy, xxz, xyz, yxz, yzy$ $yyz, yzx, zxx, zxy, zyx, zyy, zzz$	8	5	same	8 5
$2/m$	-	0	0	$xzx, xzy, xxz, xyz, yxz, yzy$ $yyz, yzx, zxx, zxy, zyx, zyy, zzz$	8 5
222	$xyz, xzy, yxz, yzx, zxy, zyx$	3	3	same	3 3
$mm2$	$xyz, xzy, yxz, yzx, zxy, zyx$	3	3	same	3 3
mmm	-	0	0	$xyz, xzy, yxz, yzx, zxy, zyx$	3 3
4	$xyz = -yxz, xzy = -yzx, xxz = yzy, xxx = yyz$ $zxx = zyy, zxy = -zyx, zzz$	4	3	same	4 3
-4	$xyz = yxz, xzy = yzx, xxz = -yzy, xxx = -yyz$ $zxx = -yzz, zxy = zyx$	4	2	$xyz = -yxz, xzy = -yzx, xxz = yzy, xxx = yyz$ $zxx = zyy, zxy = -zyx, zzz$	4 3
$4/m$	-	0	0	$xyz = -yxz, xzy = -yzx, xxz = yzy, xxx = yyz$ $zxx = zyy, zxy = -zyx, zzz$	4 3
422	$xyz = -yxz, xzy = -yzx, zxy = -zyx$	1	2	same	1 2
$4mm$	$xzx = yzy, xxx = yyz, zxx = zyy, zzz$	3	1	$xyz = -yxz, xzy = -yzx, zxy = -zyx$	1 2
-42m	$xyz = yxz, xzy = yzx, zxy = zyx$	2	1	$xyz = -yxz, xzy = -yzx, zxy = -zyx$	1 2
$4/mmm$	-	0	0	$xyz = -yxz, xzy = -yzx, zxy = -zyx$	1 2
3	$xxx = -xyy = -yyx = -yxy$ $yyy = -xxy = -xyx = -yxx$ $xxz = yyz, xzx = yzy, xyz = -yxz$ $xzy = -yzx, zxx = zyy, zxy = -zyx, zzz$	6	3	same	6 3
-3	-	0	0	$xxx = -xyy = -yyx = -yxy$ $yyy = -xxy = -xyx = -yxx$ $xxz = yyz, xzx = yzy, xyz = -yxz$ $xzy = -yzx, zxx = zyy, zxy = -zyx, zzz$	6 3
32	$xxx = -xyy = -yyx = -yxy$ $xyz = -yxz, xzy = -yzx, zxy = -zyx$	2	2	same	2 2
$3m$	$yyy = -xxy = -xyx = -yxx$ $xzx = yzy, xxx = yyz, zxx = zyy, zzz$	4	1	$xxx = -xyy = -yyx = -yxy$ $xyz = -yxz, xzy = -yzx, zxy = -zyx$	2 2
-3m	-	0	0	$xxx = -xyy = -yyx = -yxy$ $xyz = -yxz, xzy = -yzx, zxy = -zyx$	2 2
6	$xxz = yyz, xyz = -yxz, xzx = yzy,$ $xzy = -yzx, zxx = zyy, zxy = -zyx, zzz$	4	3	same	4 3
-6	$xxx = -xyy = -yyx = -yxy$ $yyy = -xxy = -xyx = -yxx$	2	0	$xxz = yyz, xyz = -yxz, xzx = yzy$ $xzy = -yzx, zxx = zyy, zxy = -zyx, zzz$	4 3
$6/m$	-	0	0	$xxz = yyz, xyz = -yxz, xzx = yzy$ $xzy = -yzx, zxx = zyy, zxy = -zyx, zzz$	4 3
622	$xyz = -yxz, xzy = -yzx, zxy = -zyx$	1	2	same	1 2
$6mm$	$xzx = yzy, xxx = yyz, zxx = zyy, zzz$	3	1	$xyz = -yxz, xzy = -yzx, zxy = -zyx$	1 2
-6m2	$yyy = -yxx = -xxy = -xyx$	1	0	$xyz = -yxz, xzy = -yzx, zxy = -zyx$	1 2
$6/mmm$	-	0	0	$xyz = -yxz, xzy = -yzx, zxy = -zyx$	1 2
23	$xyz = yzx = zxy, xzy = yxz = zyx$	1	1	same	1 1
$m-3$	-	0	0	$xyz = yzx = zxy, xzy = yxz = zyx$	1 1
432	$xyz = yzx = zxy = -xzy = -yxz = -zyx$	0	1	same	0 1
-43m	$xyz = yzx = zxy = xzy = yxz = zyx$	1	0	$xyz = yzx = zxy = -xzy = -yxz = -zyx$	0 1
$m-3m$	-	0	0	$xyz = yzx = zxy = -xzy = -yxz = -zyx$	0 1

field directions allows fine control over the direction and magnitude of the induced spin as demonstrated by the fact that the induced spin is parallel to the electric field when $\phi = 0, \pi/3, 2\pi/3, \pi$ and perpendicular at angles $\phi =$

$\pi/6, 3\pi/6, 5\pi/6, 7\pi/6, 9\pi/6, 11\pi/6$.

In Fig. 1(a) we show the spectrum of ν_2^{xxx} for Te, Se and SnS₂, computed from Density Functional Theory (DFT). For this and similar calculations, spin-orbit

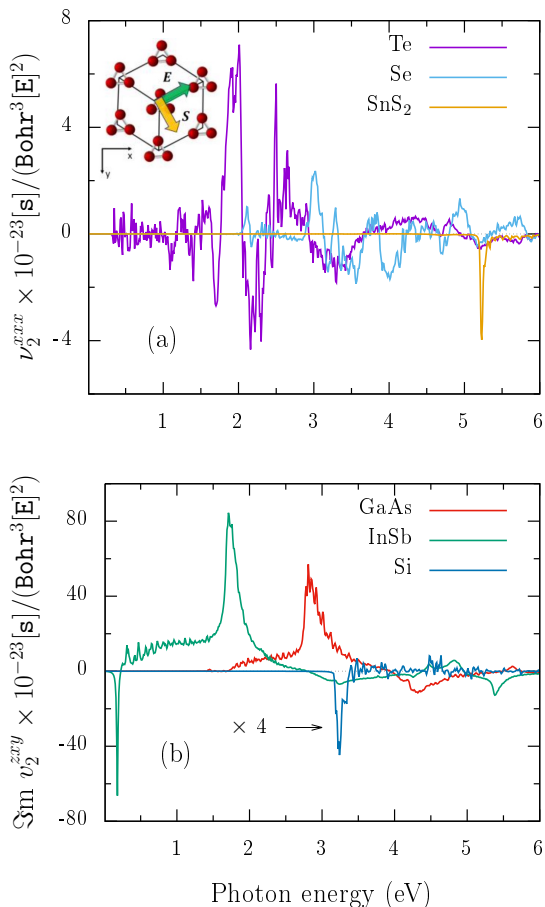


FIG. 1. (a) Spectrum of ν_2^{xxx} for Te, Se, and SnS₂. (b) Spectrum of ν_2^{zxy} for GaAs, InSb, and Si calculated using DFT. Te, Se and SnS₂ admit LPE spin polarization because $\nu_2 \neq 0$. This should be compared and contrasted with GaAs and InSb, which only admit CPE. Interestingly, SnS₂ has spin-degenerate bands at all points in the BZ and yet it exhibits a large spin polarization at 5.2 eV. Here we use $\hbar/\tau = 0.01$ eV; lattice constants and DFT band gaps are shown in Table III.

coupling is included, and thus norm-conserving relativistic separable dual-space Gaussian pseudopotentials of Hartwigsen-Goedecker-Hutter[55] are used. Furthermore, we have considered the modified Becke-Jonhson metaGGA functional[56]. To account for the under-estimation of the band gap, we have applied the scissors operator. The used scissor shifts were 0.1, 0.236 and 0.734 eV for Te, Se, and SnS₂, respectively. Convergence of spectra was reached at the cutoff energy of $E_c = 25$ Ha; 58 conduction bands for Te and Se, and 34 for SnS₂; 15062, 14256 and 14525 k -points for Te, Se and SnS₂, respectively.

–*SnS₂* (point group $-3m$): it has the same trigonal crystal system as Te and Se, and the same nonzero ν_2 and v_2 components (see Table III). But contrary to Te, SnS₂ has inversion symmetry and hence all nonlinear vector responses such as second order generation vanish. \mathcal{TI} -

symmetric materials like SnS₂ would not be expected to spin-polarized with LPE because its bands are spin-degenerate and LPE carries no angular momentum. Yet, for the same LPE as in Te, the induced spin is also given by Eq. (9). We can see from Fig. 1 (a) that it shows a comparable response as Te at 5.2 eV.

–*GaAs, InSb and Si*: GaAs and InSb (point group $-43m$) and Si (point group $m-3m$) have zinc blend and diamond structures, respectively, with only one antisymmetric component $v_2^{xyz} = v_2^{yzx} = v_2^{zxy}$ and no symmetric components. Si has inversion symmetry \mathcal{I} but GaAs and InSb do not have \mathcal{I} . It is therefore interesting to compare their CPE spin responses with the LPE spin responses of Te and SnS₂. Here, GaAs, InSb and Si spin responses reach convergence at $E_c = 20$; Ha 22, 34, and 136 conduction bands; and 75671 and 7464 k -points, correspondingly. The used scissor shifts were 0.289, 0.112 and 0.322 eV for GaAs, InSb, and Si, respectively. For a CPE in the xy -plane as $\mathbf{E} = E_0(\cos \omega t, \pm \sin \omega t, 0)$ the spin is out of plane and given by

$$\mathbf{S}^\odot = \mp \hat{\mathbf{z}} S_0^\odot, \quad (10)$$

where $S_0^\odot = i v_2^{zxy} E_0^2$ is the spin amplitude. In Fig. 1 (b) we see the spectrum of v_2^{zxy} .

Discussion: We showed that all 32 crystallography point groups admit CPE spin polarization, i.e., the usual spin orientation effects, but only 29 of those admit LPE spin polarization. CPE magnetization does not require SOC, inversion symmetry or quantum coherence. LPE magnetization on the other hand requires a not so symmetric crystal, quantum coherence and SOC. Yet, LPE has the advantage that it adds a finer control knob over the spin, namely, the electric field polarization. LPE spin-polarization although smaller, could be comparable to naturally occurring magnets hence opening available options for technological applications in magnetoptics. Note that our theory applies to the long-time limit which from experience with other nonlinear rectifying phenomena means few cycles within in a pulse in a pump probe experiment. Note also that the classification of responses using spatial groups (instead of magnetic groups) assumes weak SOC.

We illustrate these points with realistic large-scale numerical computation of prototypical semiconductors. In InSb and GaAs, CPE magnetization is an order of magnitude larger than the LPE magnetization of Te and SnS₂, (0.39 μ_B /atom vs. 0.033 μ_B /atom, see Table III). The first is comparable to iron's magnetization 2.16 μ_B /atom and the second with fcc-Ni orbital magnetization 0.053 μ_B /atom [62]. CPE and LPE both produce heating by optical absorption and possibly inducing a current [41–51]. Hence we expect LPE magnetization to be more easily observed at ultrafast times[19, 63], where quantum coherence time could be large.

TABLE III. Point groups of prototypical example materials. It is indicated if either they have \mathcal{I} or \mathcal{T} . Non-zero ν_2 and v_2 components, lattice constants, and direct band gaps are also tabulated. The maximum spin magnetization \mathcal{M}_0^{\max} is estimated from Eqs. (21) and (22) using an electric field of magnitude $E_0 = 10^9$ V/m, and the largest value of the response tensor at frequency $\hbar\omega_0$. Lattice constants and experimental band gap values are reported in the respective given references.

	Point group	\mathcal{I}	\mathcal{T}	ν_2	v_2	Lattice constants (Å)			Band gap (eV)		$ \mathcal{M}_0^{\max} $ (μ_B/atom)	$\hbar\omega_0$ (eV)
						a	b	c	DFT metaGGA	Exp.		
Te	32	\times	\checkmark	$xxx = -xyy = -yyx$ $xyz = -yzx$	$xyz = yzx$ zxy	4.46	4.46	5.93[57]	0.22 (d)	0.32 [57]	0.033	2.0
SnS ₂	-3m	\checkmark	\checkmark	$xxx = -xyy = -yyx$ $xyz = -yzx$	$xyz = yzx$ zxy	3.70	3.70	6.98	1.75 (i)	2.48[58]	0.015	5.2
GaAs	-43m	\times	\checkmark	-	$xyz = yzx = zxy$	5.65	5.65	5.65[59]	1.13 (d)	1.42-1.43[59]	0.17	2.8
InSb	-43m	\times	\checkmark	-	$xyz = yzx = zxy$	6.48	6.48	6.48 [59]	0.07 (i)	0.18[60]	0.39	1.7
Si	$m\text{-}3m$	\checkmark	\checkmark	-	$xyz = yzx = zxy$	5.43	5.43	5.43[61]	0.798 (i)	1.12[61]	0.030	3.2

Acknowledgments: BSM acknowledge support from a sabbatical fellowship and the hospitality of the Max Planck Institute for the Structure and Dynamics of Matter in Hamburg, Germany. BMF acknowledges support from NSF grant DMR-2015639.

- [1] I. Zutic, J. Fabian, and S. Das Sarma, Spintronics: Fundamentals and applications, Rev. Mod. Phys. **76**, 323 (2004).
- [2] G. Dresselhaus, Spin-orbit coupling effects in zinc blende structures, Phys. Rev. **100**, 580 (1955).
- [3] Y. A. Bychkov and E. I. Rashba, Properties of a 2d electron gas with lifted spectral degeneracy, JETP Lett. **39**, 66 (1984).
- [4] A. G. Aronov and Y. B. Lyanda-Geller, Nuclear electric resonance and orientation of carrier spins by an electric field, JETP Lett. **50**, 398 (1989).
- [5] V. Edelstein, Spin polarization of conduction electrons induced by electric current in two-dimensional asymmetric electron systems, Solid State Communications **73**, 233 (1990).
- [6] L. Pitaevskii, Electric forces in a transparent dispersive medium, Sov. Phys. JETP **12**, 1008 (1961).
- [7] F. Meier and B. P. Zakharchenya, eds., *Optical orientation, modern problems in condensed matter physics* (North Holland, Amsterdam, 1984).
- [8] H. M. van Driel and J. E. Sipe, Coherence control of photocurrents in semiconductors (Springer New York, NY, 2000) Chap. 5, pp. 261–306.
- [9] X. Zhang, Q. Liu, J.-W. Luo, A. J. Freeman, and A. Zunger, Hidden spin polarization in inversion-symmetric bulk crystals, Nature Physics volume **10**, 387–393 (2014).
- [10] J. M. Riley, F. Mazzola, M. Dendzik, M. Michiardi, T. Takayama, L. Bawden, C. Granerod, M. Leandersson, T. Balasubramanian, M. Hoesch, T. K. Kim, H. Takagi, W. Meevasana, P. Hofmann, M. Bahramy, J. Wells, and P. C. King, Direct observation of spin-polarized bulk bands in an inversion-symmetric semiconductor, Nature Physics **10**, 835 (2014).
- [11] K. Gotlieb, C.-Y. Lin, M. Serbyn, W. Zhang, C. L. Smallwood, C. Jozwiak, H. Eisaki, Z. Hussain, A. Vishwanath, and A. Lanzara, Revealing hidden spin-momentum locking in a high-temperature cuprate superconductor, Science **362**, 1271 (2018).
- [12] A. V. Kimel, A. Kirilyuk, P. A. Usachev, R. V. Pisarev, A. M. Balbashov, and T. Rasing, Ultrafast non-thermal control of magnetization by instantaneous photomagnetic pulses, nature **452**, 655 (2005).
- [13] S. A. Tarasenko, Optical orientation of electron spins by linearly polarized light, Phys. Rev. B **72**, 113302 (2005).
- [14] D. Pesin and MacDonald, Spintronics and pseudospintronics in graphene and topological insulators, Nature Mater **11**, 409–416 (2012).
- [15] C. D. Stanciu, F. Hansteen, A. V. Kimel, A. Kirilyuk, A. Tsukamoto, A. Itoh, and T. Rasing, All-optical magnetic recording with circularly polarized light, Phys. Rev. Lett. **99**, 047601 (2007).
- [16] S. Alebrand, M. Gottwald, M. Hehn, D. Steil, M. Cinchetti, D. Lacour, E. E. Fullerton, M. Aeschlimann, and S. Mangin, Light-induced magnetization reversal of high-anisotropy tbcO alloy films, Appl. Phys. Lett. **101**, 162408 (2012).
- [17] C.-H. Lambert, S. Mangin, B. S. D. C. S. Varaprasad, Y. K. Takahashi, M. Hehn, M. Cinchetti, G. Malinowski, K. Hono, Y. Fainman, M. Aeschlimann, and E. E. Fullerton, All-optical control of ferromagnetic thin films and nanostructures, Science **345**, 1337 (2014).
- [18] S. Mangin, M. Gottwald, C.-H. Lambert, D. Steil, V. Uhler, L. Pang, M. Hehn, S. Alebrand, M. Cinchetti, G. Malinowski, Y. Fainman, M. Aeschlimann, and E. E. Fullerton, Engineered materials for all-optical helicity-dependent magnetic switching, Nature Materials **13**, 286 (2014).
- [19] A. Kirilyuk, A. V. Kimel, and T. Rasing, Ultrafast optical manipulation of magnetic order, Rev. Mod. Phys. **82**, 2731 (2010).
- [20] I. D. Tokman, Q. Chen, I. A. Shereshevsky, V. I. Pozdnyakova, I. Oladyshkin, M. Tokman, and A. Belyanin, Inverse faraday effect in graphene and weyl semimetals, Phys. Rev. B **101**, 174429 (2020).
- [21] Y. Gao, C. Wang, and D. Xiao, Topological inverse faraday effect in weyl semimetals, arXiv:2009.13392 [cond-mat.mes-hall] (2020).
- [22] Y. Tanaka, T. Inoue, and M. Mochizuki, Theory of the inverse faraday effect due to the rashba spin-orbit interactions: roles of band dispersions and fermi surfaces, New Journal of Physics **22**, 083054 (2020).

- [23] S. Banerjee, U. Kumar, and S.-Z. Lin, Inverse faraday effect in mott insulators, *Phys. Rev. B* **105**, L180414 (2022).
- [24] M. Berritta, R. Mondal, K. Carva, and P. M. Oppeneer, Ab initio theory of coherent laser-induced magnetization in metals, *Phys. Rev. Lett.* **117**, 137203 (2016).
- [25] P. Scheid, G. Malinowski, S. Mangin, and S. Lebègue, Ab initio theory of magnetization induced by light absorption in ferromagnets, *Phys. Rev. B* **100**, 214402 (2019).
- [26] F. Freimuth, S. Blügel, and Y. Mokrousov, Laser-induced torques in metallic ferromagnets, *Phys. Rev. B* **94**, 144432 (2016).
- [27] O. H.-C. Cheng, D. H. Son, and M. Sheldon, Light-induced magnetism in plasmonic gold nanoparticles, *Nature Photonics* **14**, 365 (2020).
- [28] Y. Gu and K. G. Kornev, Plasmon enhanced direct and inverse faraday effects in non-magnetic nanocomposites, *J. Opt. Soc. Am. B* **27**, 2165 (2010).
- [29] J. Hurst, P. M. Oppeneer, G. Manfredi, and P.-A. Hervieux, Magnetic moment generation in small gold nanoparticles via the plasmonic inverse faraday effect, *Phys. Rev. B* **98**, 134439 (2018).
- [30] I. I. Smolyaninov, C. C. Davis, V. N. Smolyaninova, D. Schaefer, J. Elliott, and A. V. Zayats, Plasmon-induced magnetization of metallic nanostructures, *Phys. Rev. B* **71**, 035425 (2005).
- [31] M. Battiato, G. Barbalinardo, and P. M. Oppeneer, Quantum theory of the inverse faraday effect, *Phys. Rev. B* **89**, 014413 (2014).
- [32] R. Hertel, Theory of the inverse faraday effect in metals, *Journal of Magnetism and Magnetic Materials* **303**, L1 (2006).
- [33] A. Nadarajah and M. T. Sheldon, Optoelectronic phenomena in gold metal nanostructures due to the inverse faraday effect, *Opt. Express* **25**, 12753 (2017).
- [34] R. Sinha-Roy, J. Hurst, G. Manfredi, and P.-A. Hervieux, Driving orbital magnetism in metallic nanoparticles through circularly polarized light: A real-time tddft study, *ACS Photonics* **7**, 2429 (2020).
- [35] G. Wagniere, Inverse magnetochiral birefringence, *Phys. Rev. A* **40**, 2437 (1989).
- [36] P. V. Volkov and M. A. Novikov, Inverse faraday effect in anisotropic media, *Crystallography Reports* **47**, 824 (2002).
- [37] S. B. Mishra and S. Coh, Spin contribution to the inverse faraday effect of nonmagnetic metals, *Phys. Rev. B* **107**, 214432 (2023).
- [38] R. Burgos Atencia and D. Culcer, Non-conservation of the orbital moment of bloch electrons in an electric field, [arXiv:2311.12108](https://arxiv.org/abs/2311.12108) [cond-mat.mes-hall].
- [39] B. M. Fregoso, Bulk photospin effect: Calculation of electric spin susceptibility to second order in an electric field, *Phys. Rev. B* **106**, 195108 (2022).
- [40] R. W. Boyd, *Nonlinear Optics* (Academic Press, 2008).
- [41] B. I. Sturman and P. J. Sturman, *Photovoltaic and Photo-refractive Effects in Noncentrosymmetric Materials* (CRC Press, 1992).
- [42] R. von Baltz and W. Kraut, Theory of the bulk photovoltaic effect in pure crystals, *Phys. Rev. B* **23**, 5590 (1981).
- [43] J. E. Sipe and A. I. Shkrebtii, Second-order optical response in semiconductors, *Phys. Rev. B* **61**, 5337 (2000).
- [44] B. M. Fregoso, Bulk photovoltaic effects in the presence of a static electric field, *Phys. Rev. B* **100**, 064301 (2019).
- [45] J. Ibanez-Azpiroz, S. S. Tsirkin, and I. Souza, Ab initio calculation of the shift photocurrent by wannier interpolation, *Phys. Rev. B* **97**, 245143 (2018).
- [46] T. Holder, Electrons flow like falling cats: Deformations and emergent gravity in quantum transport, [arXiv:2111.07782](https://arxiv.org/abs/2111.07782) [cond-mat.mes-hall] (2021).
- [47] Q. Ma, A. G. Grushin, and K. S. Burch, Topology and geometry under the nonlinear electromagnetic spotlight, *Nature Materials* **20**, 1601 (2021).
- [48] J. Ahn, G.-Y. Guo, N. Nagaosa, and A. Vishwanath, Riemannian geometry of resonant optical responses, *Nature Physics* **18**, 290–295 (2022).
- [49] A. Alexandradinata and P. Zhu, Anomalous shift and optical vorticity in the steady photovoltaic current, [arXiv:2308.08596](https://arxiv.org/abs/2308.08596) [cond-mat.mes-hall] (2023).
- [50] W. J. Jankowski, A. S. Morris, A. Bouhon, F. N. Unal, and R.-J. Slager, Optical manifestations of topological euler class in electronic materials, [arXiv:2311.07545](https://arxiv.org/abs/2311.07545) [cond-mat.mes-hall] (2023).
- [51] R. Resta, Geometrical theory of the shift current in presence of disorder and interaction, [arXiv:2402.12489](https://arxiv.org/abs/2402.12489) [cond-mat.mtrl-sci] (2024).
- [52] F. Nastos and J. E. Sipe, Optical rectification and shift currents in gaas and gap response: Below and above the band gap, *Phys. Rev. B* **74**, 035201 (2006).
- [53] J. Rioux and J. Sipe, Optical injection processes in semiconductors, *Physica E: Low-dimensional Systems and Nanostructures* **45**, 1 (2012).
- [54] N. Ofer, T.-D. Nicolas, D. G. Umberto, H. Hannes, and R. Angel, Attosecond magnetization dynamics in non-magnetic materials driven by intense femtosecond lasers, *npj Computational Materials* **9**, 39 (2023).
- [55] C. Hartwigsen, S. Goedecker, and J. Hutter, Relativistic separable dual-space gaussian pseudopotentials from H to Rn, *Phys. Rev. B*.
- [56] E. Räsänen, S. Pittalis, and C. R. Proetto, Universal correction for the becke–johnson exchange potential, *The Journal of Chemical Physics* **132**, 044112 (2010).
- [57] V. Orlov and G. S. Sergeev, Electronic band structure and chemical bonding in trigonal Se and Te, *AIP Advances* **12**, 055110 (2022).
- [58] L. A. Burton, T. J. Whittles, D. Hesp, W. M. Linhart, J. M. Skelton, B. Hou, R. F. Webster, G. O’Dowd, C. Reece, D. Cherns, D. J. Fermin, T. D. Veal, V. R. Dhanak, and A. Walsh, Electronic and optical properties of single crystal SnS₂: an earth-abundant disulfide photocatalyst, *J. Mater. Chem. A* **4**, 1312 (2016).
- [59] J. R. M. I. Vurgaftman and L. R. Ram-Mohan, Band parameters for III–V compound semiconductors and their alloys, *Journal of Applied Physics* **89**, 5815 (2001).
- [60] S. Adachi, *Optical Constants of Crystalline and Amorphous Semiconductors* (Kluwer Academic Publishers, 1999).
- [61] S. M. Sze and K. K. Ng, *Physics of Semiconductor Devices, 3rd. edition* (John Wiley & Sons, Inc., 2007).
- [62] T. Thonhauser, Theory of orbital magnetization in solids, *International Journal of Modern Physics B* **25**, 1429 (2011).
- [63] O. Busch, F. Ziolkowski, I. Mertig, and J. Henk, Ultrafast dynamics of electrons excited by femtosecond laser pulses: Spin polarization and spin-polarized currents, *Phys. Rev. B* **108**, 184401 (2023).

SUPPLEMENTARY INFORMATION

Theory of LPE and CPE spin polarization

We consider an insulator with fully occupied valence bands and fully empty conduction bands. Let us assume there is a monochromatic optical field of the form $\mathbf{E} = \mathbf{E}(\omega)e^{-i\omega t} + \text{c.c.}$. The *static* induced spin to second order in the electric field is

$$S^a = 2\zeta^{abc}(0; \omega, -\omega)E^b(\omega)E^c(-\omega). \quad (11)$$

We now separate the symmetric and antisymmetric responses of the *interband* response by defining

$$\nu_2^{abc} \equiv (\zeta^{abc} + \zeta^{acb})/2, \quad (12)$$

$$v_2^{abc} \equiv (\zeta^{abc} - \zeta^{acb})/2. \quad (13)$$

Eq. (11) then becomes

$$S^{(2)a} = 2\nu_2^{abc}E^b(\omega)E^c(-\omega) + 2v_2^{abc}E^b(\omega)E^c(-\omega), \quad (14)$$

which is of the form of Eq. (6). The tensor ζ^{abc} can be further decomposed into 2-band and 3-band contributions,^[39]

$$\zeta = \zeta_{2b} + \zeta_{3b}, \quad (15)$$

where

$$\zeta_{2b}^{abc} = -\frac{ie^2}{2\hbar^2V} \sum_{nm\mathbf{k}} \frac{s_{nm}^a}{\bar{\omega}_{nm}} \left[\left(\frac{r_{mn}^b f_{nm}}{\omega_{mn} - \bar{\omega}} \right)_{;c} + \left(\frac{r_{mn}^c f_{nm}}{\omega_{mn} + \bar{\omega}^*} \right)_{;b} \right], \quad (16)$$

$$\zeta_{3b}^{abc} = \frac{e^2}{2\hbar^2V} \sum_{nm\mathbf{k}} \frac{s_{nm}^a}{\bar{\omega}_{nm}} \left[\frac{r_{ml}^b r_{ln}^c f_{lm}}{\omega_{ml} - \bar{\omega}} - \frac{r_{ml}^c r_{ln}^b f_{ln}}{\omega_{ln} - \bar{\omega}} + \frac{r_{ml}^c r_{ln}^b f_{lm}}{\omega_{ml} + \bar{\omega}^*} - \frac{r_{ml}^b r_{ln}^c f_{ln}}{\omega_{ln} + \bar{\omega}^*} \right], \quad (17)$$

and $\bar{\omega} \equiv \omega + i/\tau$ and $\bar{\omega}_{nm} = \omega_{nm} + i/\tau$. The notation used is the same as in ^[39]. Although not obvious, ν_2 depends on the off-diagonal elements of density matrix whereas v_2 depends on the diagonal elements of the density matrix. It is easy to check that $(\zeta^{abc})^* = \zeta^{acb}$ and hence

$$\nu_2 = \text{Re}[\zeta], \quad (18)$$

$$v_2 = i\text{Im}[\zeta]. \quad (19)$$

These equations are used to compute ν_2 and v_2 in the main text.

Magnetic Moment

With the help of Eqs. (18) and (19), it is possible to obtain the magnetization due to the electron spin, which is proportional to the spin polarization \mathbf{S} of the sample per unit volume. Thus the magnetization per unit cell volume V_{ucell} and per unit atom is written as

$$\mathcal{M} = 2\mu_B \frac{\mathbf{S}}{\hbar} \frac{V_{\text{ucell}}}{N}, \quad (20)$$

where μ_B is the Bohr magneton and N the number of atoms in the unit cell. For LPE in the xy -plane, the magnitude of the magnetization is written as

$$\mathcal{M}_0^{\leftrightarrow} = 2\mu_B \frac{S_0^{\leftrightarrow}}{\hbar} \frac{V_{\text{ucell}}}{N}, \quad (21)$$

with $S_0^{\leftrightarrow} = E_0^2 \nu_2^{xxx}/2$. While for a CPE in the xy -plane and for crystals with only antisymmetric components, it is out of plane and given by

$$\mathcal{M}_0^{\circ} = \mp 2\mu_B \frac{S_0^{\circ}}{\hbar} \frac{V_{\text{ucell}}}{N}, \quad (22)$$

with $S_0^{\circ} = iv_2^{zxy} E_0^2$.

Symmetric and antisymmetric pseudo-tensor components

TABLE IV. Symmetric σ_2 (ν_2) and antisymmetric η_2 (v_2) decomposition of the nonzero components of the 3rd-rank tensor (pseudotensor).

Point group	tensor		pseudo-tensor	
	σ_2	η_2	ν_2	v_2
1	$xxx, xyy, xzz, yxx, yyy, yzz$ $zxx, zyy, zzz, xxy, xxz, xyz$ $yxy, yxz, yyz, zxy, zxz, zyz$	xyx, xxz, xyz, yxy yxz, yyz, zxy, zxz zyz	same	same
-1	-	-	$xxx, xyy, xzz, yxx, yyy, yzz$ $zxx, zyy, zzz, xxy, xxz, xyz$ $yxy, yxz, yyz, zxy, zxz, zyz$	xyx, xxz, xyz, yxy yxz, yyz, zxy, zxz zyz
2	xzx, xzy, yxz, yyz zxx, zxy, zyy, zzz	xzx, xzy, yxz yyz, zxy	same	same
m	xzx, xzy, yxz, yyz zxx, zxy, zyy, zzz	xzx, xzy, yxz yyz, zxy	same	same
$2/m$	-	-	xzx, xzy, yxz, yyz zxx, zxy, zyy, zzz	xzx, xzy, yxz yyz, zxy
222	xyz, yxz, zxy	xyz, yxz, zxy	same	same
$mm2$	xyz, yxz, zxy	xyz, yxz, zxy	same	same
mmm	-	-	xyz, yxz, zxy	xyz, yxz, zxy
4	$xyz = -yxz, xzx = yzy$ $zxx = zyy, zzz$	$xyz = -yxz, xzx = yzy$ zxy	same	same
-4	$xyz = yxz, xzx = -yzy$ $zxx = -yzz, zxy = zyx$	$xyz = yxz$ $xzx = -yzy$	$xyz = -yxz, xzx = yzy$ $zxx = zyy, zzz$	$xyz = -yxz, xzx = yzy$ zxy
$4/m$	-	-	$xyz = -yxz, xzx = yzy$ $zxx = zyy, zzz$	$xyz = -yxz, xzx = yzy$ zxy
422	$xyz = -yxz$	$xyz = -yxz, zxy$	same	same
$4mm$	$xzx = yzx, zxx = zyy$ zzz	$xzx = yzy$	$xyz = -yxz$	$xyz = -yxz$ zxy
-42m	$xyz = yxz, zxy$	$xyz = yxz$	$xyz = -yxz$	$xyz = -yxz, zxy$
$4/mmm$	-	-	$xyz = -yxz$	$xyz = -yxz, zxy$
3	$xxx = -xyy = -yyx$ $yyy = -xxy = -xyx$ $xxz = yyz, xyz = -yxz$ $zxx = zyy, zzz$	$xxz = yyz, xyz = -yxz$ zxy	same	same
-3	-	-	$xxx = -xyy = -yyx$ $yyy = -xxy = -xyx$ $xxz = yyz, xyz = -yxz$ $zxx = zyy, zzz$	$xxz = yyz, xyz = -yxz$ zxy
$4mm$	$xzx = yzx, zxx = zyy$ zzz	$xzx = yzy$	$xyz = -yxz$	$xyz = -yxz$ zxy
32	$xxx = -xyy = -yyx$ $xyz = -yxz$	$xyz = -yxz$ xzy	same	same
$3m$	$yyy = -xxy = -yyx$ $xzx = yzy, zxx = zyy, zzz$	$xzx = yzy$	$xxx = -xyy = -yyx$ $xyz = -yxz$	$xyz = -yxz$ zxy
-3m	-	-	$xxx = -xyy = -yyx$ $xyz = -yxz$	$xyz = -yxz$ zxy
6	$xxz = yyz, xyz = -yxz$ $zxx = zyy, zzz$	$xxz = yyz, xyz = -yxz$ zxy	same	same
-6	$xxx = -xyy = -yyx$ $yyy = -xxy = -yyx$	-	$xxz = yyz, xyz = -yxz$ $zxx = zyy, zzz$	$xxz = yyz, xyz = -yxz$ zxy
$6/m$	-	-	$xxz = yyz, xyz = -yxz$ $zxx = zyy, zzz$	$xxz = yyz, xyz = -yxz$ zxy
622	$xyz = -yxz$	$xyz = -yxz, zxy$	same	same
$6mm$	$xzx = yzy, zxx = zyy, zzz$	$xzx = yzy$	$xyz = -yxz$	$xyz = -yxz, zxy$
-6m2	$yyy = -yxx = -xxy$	-	$xyz = -yxz$	$xyz = -yxz, zxy$
$6/mmm$	-	-	$xyz = -yxz$	$xyz = -yxz, zxy$
23	$xyz = yzx = zxy$	$xyz = yzx = zxy$	same	same
$m-3$	-	-	$xyz = yzx = zxy$	$xyz = yzx = zxy$
432	-	$xyz = yzx = zxy$	same	same
-43m	$xyz = yzx = zxy$	-	-	$xyz = yzx = zxy$
$m-3m$	-	-	-	$xyz = yzx = zxy$